MICROWAVE IMAGING OF THREE-DIMENSIONAL DIELECTRIC OBJECTS

Tony HUANG, and Ananda S. MOHAN
Microwave and Wireless Technology Research Laboratory, ICT Group,
Faculty of Engineering, University of Technology, Sydney (UTS)
PO Box 123, Broadway, N.S.W. 2007, Australia
E-mail: thuang@eng.uts.edu.au; ananda@eng.uts.edu.au

1. Introduction

Microwave imaging is an electromagnetic (EM) inverse scattering application that has played an important role in various fields such as radar, remote sensing and biomedical applications. By subjecting the object under investigation (OUI) to microwave radiation, the measured scattered fields are used to produce images which are maps of spatial distributions of EM profiles inside the OUI.

However, for penetrable dielectric objects, especially the heterogeneous case, the incident wave is scattered in all directions and is likely to undergo multiple reflections. Therefore the measured scattered fields do not possess a linear relationship with the spatial distribution of dielectric properties inside the OUI. To further complicate the situation, the evanescent waves are not measured and the high spatial frequency information is lost as the result of this. Hence the process of reconstructing microwave images is a difficult task as it needs to solve a complex EM inverse scattering problem.

In general, this nonlinear and strongly ill-posed problem is often being modeled as a global optimization problem and is solved by iterative techniques such as Newton-Kantorovitch method (NKM) [1] and modified gradient method (MGM) [2]. At each iterative process, the measured scattered field is compared with the scattered field computed from the numerical model of OUI and EM profiles of the model is then progressively adjusted by minimizing the error between these two sets of data. It has been shown in many publications that both NKM and MGM can be successfully applied to solve two-dimensional (2-D) problems, but for three-dimensional (3-D) cases the work reported in the literature are quite limited [3], [4]. The difficulty involved in applying NKM and MGM to 3-D problems are caused by the requirement of an accurate initial estimate of the OUI. As both NKM and MGM are based on the deterministic optimization methods (DOMs), without an accurate initial estimate, the solution could get trapped in a local minimum. In addition, an inversion of large dimensional matrices is required for NKM, which makes it even more difficult to be applied in practical 3-D cases. To bypass the difficulties presented in these techniques, inversion algorithms that are based on the stochastic optimization methods (SOMs) such as genetic algorithm (GA), simulated annealing (SA) and artificial neural networks (ANN) have been proposed [5]-[7].

In this paper we consider the use of micro-genetic algorithm (m-GA), an enhancement to the conventional GA, to the reconstruction of microwave images of 3-D dielectric objects. The paper is organized as follows. In section 2, the formulation of 3-D microwave imaging problem is presented along with the description of m-GA and its application on solving the inverse scattering problem. In Section 3, we provide some simulation results of the reconstructed images, and finally the conclusion is presented in Section 4.

2. Theoretical Formulation

For 3-D heterogeneous scatterers, the scattered field can be computed using volume integral equations. We let $\vec{E}, \vec{E}^i$ and $\vec{E}^s$ denotes the total field, incident field and scattered field, respectively and $\vec{E} = \vec{E}^i + \vec{E}^s$. Suppose a 3-D dielectric scatterer is characterized by its complex permittivity, ε, which is defined by $\varepsilon = (\varepsilon_r - j\sigma / \omega\varepsilon_0)\varepsilon_0$. By using the volumetric equivalence principle, the dielectric scatterer may be replaced by an equivalent electric current density radiating in free space, i.e.

$$\vec{J} = j\omega(\varepsilon - \varepsilon_0)\vec{E} = j\omega(\varepsilon - \varepsilon_0)\left[\vec{E}^i + \vec{E}^s\right] \tag{1}$$

The scattered field $\vec{E}^s$ produced by $\vec{J}$ can then be expressed as

$$\vec{E}^s = -\frac{j\omega\mu_0}{4\pi}\iiint_V \vec{J}G dV - \frac{\vec{\nabla}}{j\omega 4\pi\varepsilon_0}\iint_S (\hat{n}\cdot\vec{J})G dS \tag{2}$$

where $\hat{n}$ is a unit outward normal vector to the surface of the scatterer and G is the Green's function defined by

$$G = \frac{e^{-jkR}}{R} \tag{3}$$

where $R = \sqrt{(x-x')^2 + (y-y')^2 + (z-z')^2}$ and k is the wave number.

By using (1) and (2) we can relate the unknown current density $\vec{J}$ to the known incident field $\vec{E}^i$ and obtain the expression below

$$\vec{E}^i = \frac{\vec{J}}{j\omega(\varepsilon - \varepsilon_0)} + \frac{j\omega\mu_0}{4\pi}\iiint_V \vec{J}G dV + \frac{\vec{\nabla}}{j\omega 4\pi\varepsilon_0}\iint_S (\hat{n}\cdot\vec{J})G dS \tag{4}$$

After the current density $\vec{J}$ is determined from (4), secondary quantities of interest such as the scattered field and bistatic radar cross section can be easily computed.

This procedure of calculating the EM field with given source and spatial distribution of dielectric properties of the scatterer is called the forward scattering problems. On the other hand, the inverse scattering problems requires to the procedure of finding the spatial distribution of dielectric properties of the scatterer from a known source as well as the measured EM field values on receivers.

In this paper, we are interested in applying m-GA to solve the 3-D inverse scattering problem. As mentioned in the introduction, m-GA is an enhancement to the conventional GA. Like GA, it is also a stochastic optimization technique that is based on Darwin's theory of natural evolution. With m-GA, it does not employ a large population size like the conventional GA and it is capable of preventing premature convergence for the solution while assuring a rapid convergence rate to the near-optimal regions.

To solve the 3-D inverse scattering problem, we first assume the OUI is contained inside an investigation domain and the investigation domain is partitioned into a number of sub-volumes. The dielectric property of each sub-volume is assumed to be constant. The field scattered by the OUI is measured at the observation planes, which in this case is located outside the investigation domain.

We start by generating some investigation domains with random dielectric properties for the sub-volumes. These investigation domains are then encoded into a set of binary strings for the formation of m-GA population. The population of m-GA will undergo the usual selection and crossover process as with the conventional GA, but omitting the mutation operation. Instead of the mutation operation, it uses a population restart scheme to maintain its population diversity and at the same time elitist operator is applied to ensure the fittest individual is migrated from one generation to the next. The goal here is to apply m-GA to minimize the discrepancy between the measured and computed values of the scattered field. Therefore, we define the cost function (CF) of m-GA as the normalized root mean square error between the measured and computed values of $\vec{E}^s$, i.e.

$$CF = \sqrt{\frac{1}{V}\sum_{v=1}^{V} \frac{\left|E_{meas}^s(\rho_v) - E_{comp}^s(\rho_v)\right|^2}{\left|E_{meas}^s(\rho_v)\right|^2}} \tag{5}$$

where V, $E_{meas}^s(\rho_v)$ and $E_{comp}^s(\rho_v)$ are the total number of measurement points, measured and computed values of $\vec{E}^s$ at location ρ_v, respectively.

3. Simulation Results

To demonstrate the use of m-GA in solving 3-D microwave image reconstruction problems, we have considered the scenario described in the first example of [4]. In this particular case, a cubic region of side length λ_0 is considered as the investigation domain, where λ_0 is the wavelength in free space. The investigation domain is partitioned into 27 cubic cells (side length = $\lambda_0/3$) and one of the cell is occupied by the OUI, as illustrated in Fig. 1. The OUI considered in this computer simulation is a homogeneous lossless scatterer, characterized by a relative dielectric permittivity $\varepsilon_r = 6$.

Outside the cubic investigation domain there are six observation planes parallel to each surface of the investigation domain. Each observation plane has 49 measurement points equally spaced over an area of $\lambda_0 \times \lambda_0$, and the distance between the centre of the investigation domain and each observation plane is equal to λ_0. Fig. 2 shows the horizontal cross-sectional view of this arrangement.

The investigation domain is illuminated by a plane wave of incident frequency $f_0 = 2.45\text{GHz}$. The incident plane wave is propagating along the z-axis, while the electric field vector is polarized along the y-axis.

For the implementation of m-GA, we have used 5 chromosomes to make up the m-GA population, i.e. $N_{pop} = 5$, and for each chromosome there are 27 genes representing the relative dielectric permittivity of the sub-volumes for the investigation domain, i.e. $N_{gene} = 27$. Other assumed parameters are: N_{bit} (Number of bits per gene) = 4, P_c (probability of crossover) = 0.8, P_{th} (convergence threshold for initiating the population restart scheme) = 0.9. The m-GA is set to terminate its iterative process when $CF \le 0.005$ or N_{it} (number of iterations) = 1500.

Also, to investigate the effect of noise, additive white Gaussian noise is added to the synthetic measured data, and Figs. 3(a)-(c) shows the reconstructed spatial distribution of ε_r for the three layers of the investigation domain when SNR = 20dB.

From the results shown in Figs. 3(a)-(c), it is clear that m-GA have successfully determined the spatial distribution of ε_r inside the investigation domain with reasonable accuracy, and a significant contrast in ε_r between the scatterer cell and other empty cells can also be visualized.

4. Conclusion

In this paper, we have successfully demonstrated the use of m-GA to reconstruct microwave images that shows the spatial distribution of dielectric properties for 3-D dielectric objects. We have obtained excellent results on dielectric reconstructions though our simulations and we are currently investigating the potentialities of this technique for other microwave imaging applications.

Reference
[1] A. E. Souvorov, A. E. Bulyshev, S. Y. Semenov, R. H. Svenson, A. G. Nazarov, Y. E. Sizov, and G. P. Tatsis, "Microwave tomography: A two-dimensional Newton iterative scheme," *IEEE Trans. Microwave Theory Tech.*, vol. 46, pp. 1654-1659, 1998.
[2] R. E. Kleinman and P. M. van den Berg, "A modified gradient method for two-dimensional problems in tomography," *J. Comput. Appl. Math.*, vol.42, pp. 17-35, 1992.
[3] N. Joachimovitz, C. Pichot, and J. P. Hugonin, "Inverse scattering: An iterative numerical method for electromagnetic imaging," *IEEE Trans. Antennas Propagat.*, vol. 39, pp. 1742-1751, 1991.
[4] S. Caorsi, G. L. Gragnani, and M. Pastorino, "Redundant electromagnetic data for microwave imaging of three-dimensional dielectric objects," *IEEE Trans. Antennas Propagat.*, vol. 42, pp. 581-589, 1994

[5]   M. Pastorino, A. Massa, and S. Caorsi, "A microwave inverse scattering technique for image reconstruction based on a genetic algorithm," *IEEE Trans. Instrum. Meas.*, vol. 49, pp.573-578, 2000.

[6]   S. Caorsi, G. L. Gragnani, S. Medicina, M. Pastorino, and G. Zunino, "Microwave imaging method using a simulated annealing approach," *IEEE Microwave Guided Wave Lett.*, vol. 1, pp. 331-333, 1991.

[7]   E. Bermani, S. Caorsi, and M. Raffetto, "Microwave detection and dielectric characterization of cylindrical objects from amplitude-only data by means of neural networks," *IEEE Trans. Antennas Propagat.*, vol. 50, pp. 1309-1314, 2002.
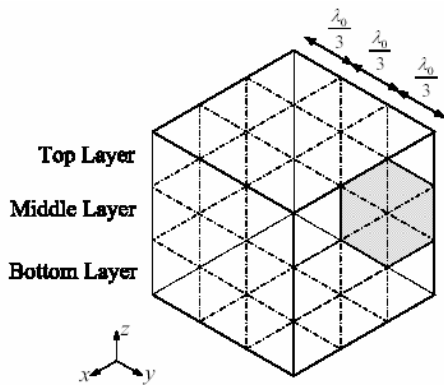
Fig. 1. The cubic investigation domain is partitioned into 27 sub-volumes. The shaded area indicates the dielectric scatterer.
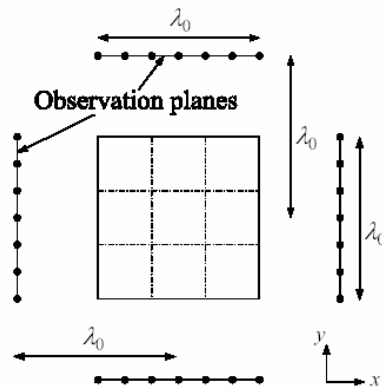
Fig. 3(b) Spatial distribution of ε_r for the middle layer of the investigation domain. SNR = 20dB.

Fig. 2. Horizontal cross-sectional view of the arrangements for the investigation domain and observation planes.

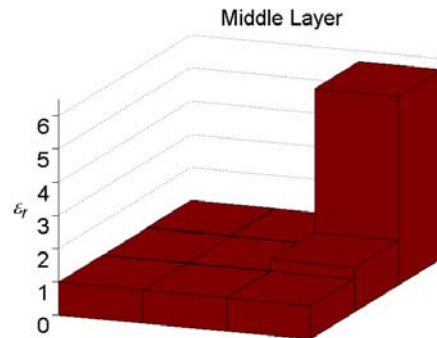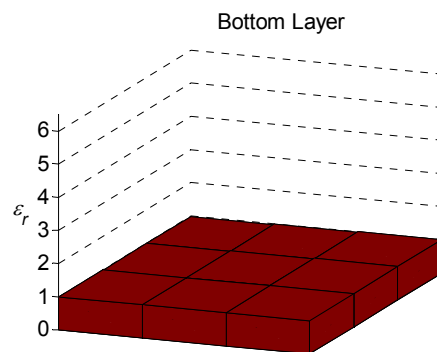Fig. 3(c) Spatial distribution of ε_r for the bottom layer of the investigation domain. SNR = 20dB.

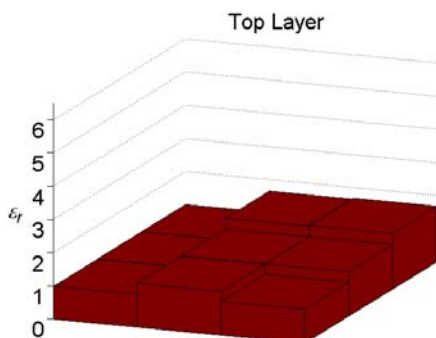Fig. 3(a) Spatial distribution of ε_r for the top layer of the investigation domain. SNR = 20dB.